Hydraulic Engineering Software VIII, C.A. Brebbia & W.R. Blain (Editors)

Inundation flow modeling in urban area based on the unstructured meshes

K. Kawaike[1], K. Inoue[2] & K. Toda[2]
[1]*Department of Civil Engineering, Kyoto University, Japan.*
[2]*Disaster Prevention Research Institute, Kyoto University, Japan.*

Abstract

An advanced inundation flow model based on the unstructured meshes is newly developed, which can treat suitably the shapes of linear structures such as small rivers and continuous banking. In this model, small rivers can be treated as rectangular channels which comprise a series of meshes with lower elevation and continuous banking can be treated as linear boundary walls. From the obtained results it can be concluded that this model can evaluate the influence of small rivers and continuous banking successfully and can be applicable for inundation flow prediction in urban area.

1 Introduction

In most of the existing inundation flow models, the Cartesian coordinate system has been adopted because of its easiness of mesh generation [1]. This coordinate system is, however, difficult to treat a various kinds of factors in urban area, such as streets, buildings, small rivers or continuous banking, which have much influence to the inundation water behavior. In order to take these factors in urban area into account, the inundation flow model by the unstructured meshes is developed here, which can divide the computational region into arbitrary-shaped meshes. Especially, this model aims to treat the linear structures such as small rivers and continuous banking suitably.

2 Numerical Simulation Method

The governing equations used here are the following continuity equation and

Hydraulic Engineering Software VIII, C.A. Brebbia & W.R. Blain (Editors)

the momentum equations.

$$\frac{\partial h}{\partial t} + \frac{\partial M}{\partial x} + \frac{\partial N}{\partial y} = 0 \tag{1}$$

$$\frac{\partial M}{\partial t} + \frac{\partial (uM)}{\partial x} + \frac{\partial (vM)}{\partial y} = -gh\frac{\partial H}{\partial x} - \frac{gn^2 M\sqrt{u^2+v^2}}{h^{4/3}} \tag{2}$$

$$\frac{\partial N}{\partial t} + \frac{\partial (uN)}{\partial x} + \frac{\partial (vN)}{\partial y} = -gh\frac{\partial H}{\partial y} - \frac{gn^2 N\sqrt{u^2+v^2}}{h^{4/3}} \tag{3}$$

where t is time, x and y are rectangular coordinates, h is water depth, M, N are x- and y- components of discharge flux, respectively, u, v are x- and y- components of velocity, respectively, H is water stage and n is roughness coefficient.

However, meshes used here are constituted by polygons. As for the location of unknown values, water depth is defined at a centroid of mesh (a centroid of polygon in this study) and discharge flux and velocity are defined at the middle point of side of polygon.

In the continuity equation, a polygon mesh is treated as a control volume (see Figure 1), and the following finite difference equation is used;

$$\frac{h^{n+3} - h^{n+1}}{2\Delta t} + \frac{1}{A}\sum_{l=1}^{m}\left\{M_l^{n+2}(\Delta y)_l - N_l^{n+2}(\Delta x)_l\right\} = 0 \tag{4}$$

where superscripts denote the time step, A is area of the control volume and m is the number of sides which surround the control volume. $(\Delta x)_l$ and $(\Delta y)_l$ are the difference of the x and y coordinates at both ends of side l, respectively.

As for the momentum equations, in the computation on the border line L adjacent to mesh i and mesh j, the following finite difference equation is applied by use of the variables shown in Figure 2;

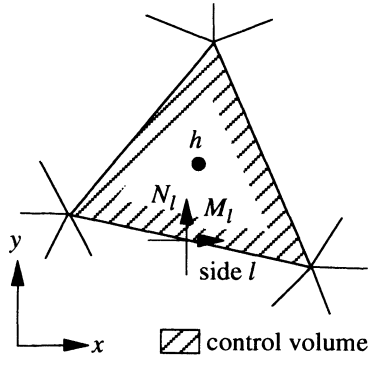

Figure 1: Control volume for continuity equation

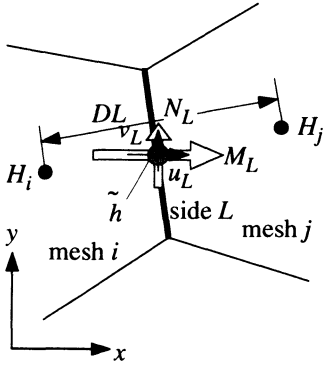

Figure 2: Treatment of momentum equation

Hydraulic Engineering Software VIII, C.A. Brebbia & W.R. Blain (Editors)

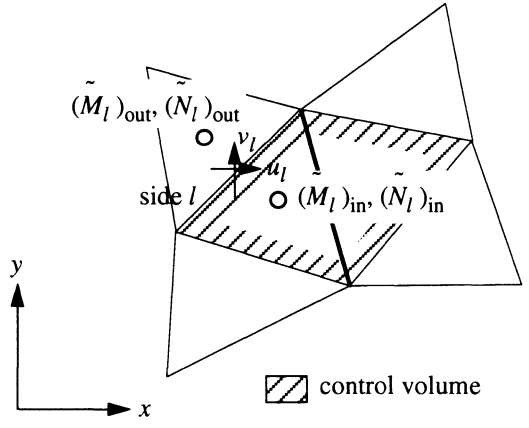

Figure 3: Control volume for calculation of convective term

$$\frac{M_L^{n+2} - M_L^n}{2\Delta t} + M1 + M2 = -g\tilde{h}^{n+1}(\nabla H)_x - \frac{gn^2 \frac{M_L^{n+2}+M_L^n}{2}\sqrt{(u_L^n)^2 + (v_L^n)^2}}{(\tilde{h}^{n+1})^{4/3}} \tag{5}$$

$$\frac{N_L^{n+2} - N_L^n}{2\Delta t} + N1 + N2 = -g\tilde{h}^{n+1}(\nabla H)_y - \frac{gn^2 \frac{N_L^{n+2}+N_L^n}{2}\sqrt{(u_L^n)^2 + (v_L^n)^2}}{(\tilde{h}^{n+1})^{4/3}} \tag{6}$$

where M_L, N_L and u_L, v_L are the discharge fluxes and the velocity components on the border line L, respectively, $\tilde{h}$ is the interpolated water depth on the line L and $(\nabla H)_x$ and $(\nabla H)_y$ are x- and y- component of water surface gradient between the mesh i and mesh j, respectively. $M1 + M2$, $N1 + N2$ are the convective terms, which are expressed by the following equations;

$$M1 + M2 = \frac{1}{A_{cv}} \sum_{l=1}^{m'} \left\{ (u_l \tilde{M}_l)(\Delta y)_l - (v_l \tilde{M}_l)(\Delta x)_l \right\} \tag{7}$$

$$N1 + N2 = \frac{1}{A_{cv}} \sum_{l=1}^{m'} \left\{ (u_l \tilde{N}_l)(\Delta y)_l - (v_l \tilde{N}_l)(\Delta x)_l \right\} \tag{8}$$

where A_{cv} is the area of control volume which denotes the two meshes adjacent to the line L (see Figure 3), m' is the number of sides which surround the control volume and $\tilde{M}_l$ and $\tilde{N}_l$ are the interpolated discharge flux on the centroid of the mesh. The upstream side of $\tilde{M}$ and $\tilde{N}$ are chosen depending on the direction of u_l and v_l.

3 Application of the model to the Tone river basin

The model described in the above section is applied to the Tone river basin

Hydraulic Engineering Software VIII, C.A. Brebbia & W.R. Blain (Editors)

which covers the east of Saitama prefecture and Adachi Ward, Katsushika Ward and Edogawa Ward of the city of Tokyo (see Figure 4). This area suffered a heavy flood damage due to the bank breaking of the Tone river in 1947. Figure 5 [2] shows the inundation record at that time. This area also includes rivers such as the Naka river and the Ayase river which run in the city area and linear structures such as railway and highway.

In computation, the same bank breaking point as that in 1947 is assumed, from which the river water is supposed to flow into the bank protected area according to the hydrograph in Figure 6 [2].

First, in order to compare the result by the unstructured meshes with that by the existing Cartesian meshes, a simple computational condition is adopted in which the effects of small rivers and linear structures are not considered. Figure 7 shows both the Cartesian coordinate meshes and the unstructured meshes used in this study. The surface elevation distribution is also shown in the figure of Cartesian coordinate. The Manning coefficient n used here is n=0.067. Figure 8 and Figure 9 show the computational results by the Cartesian coordinate meshes and by the un-

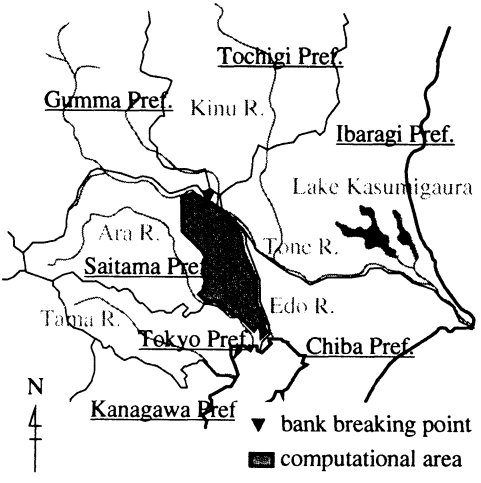

Figure 4: Computational area

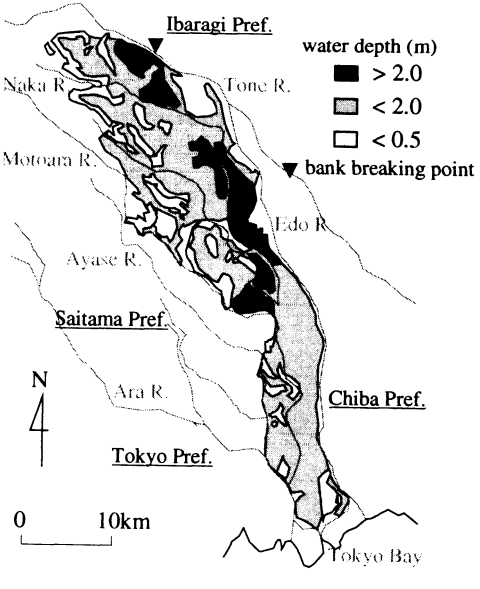

Figure 5: Inundation area in 1947

Hydraulic Engineering Software VIII, C.A. Brebbia & W.R. Blain (Editors)

structured meshes, respectively. It is seen that in this simplified condition, the model proposed here can produce almost the similar result with that by the existing model. But it is also seen that if this result is compared with the inundation record in 1947, the computed inundation depth at downstream area becomes higher and the inundation area extends to the west more than the record. This is by the reason that in this model, the downstream boundary is assumed to be a high wall and the inundation water drainage is not taken into consideration. Actually, a large amount of inundation water is expected to flow out through small rivers.

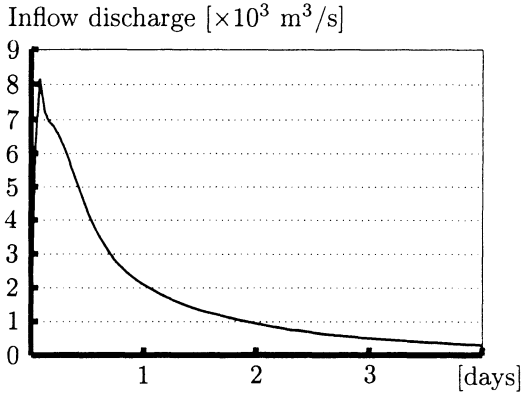

Figure 6: Inflow discharge hydrograph

Next, the computation by the unstructured meshes with consideration of small river effect is conducted. The studied area comprises the meshes of small rivers and those of flood plain. Figure 10 shows the rivers taken as small rivers in the studied area. These rivers are treated as dug channels with rectangular cross-section whose bed elevation is lower than the neighboring surface. The dug depth is determined by the river cross-section data

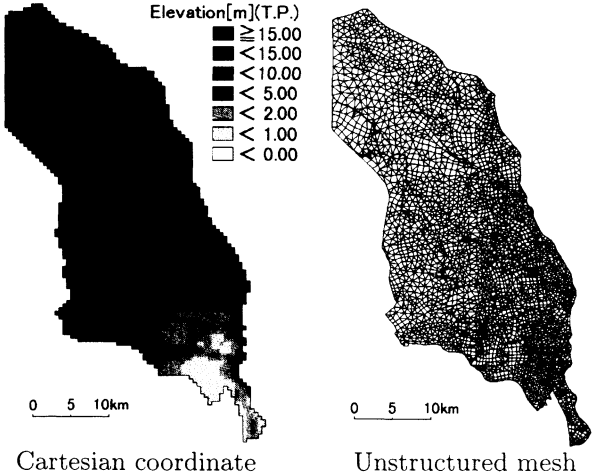

Figure 7: Computational meshes and elevation

Hydraulic Engineering Software VIII, C.A. Brebbia & W.R. Blain (Editors)

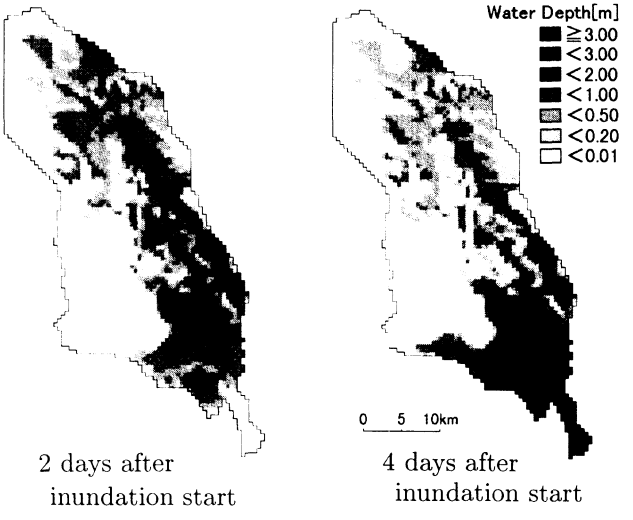

Figure 8: Temporal change of water depth (Cartesian coordinate meshes)

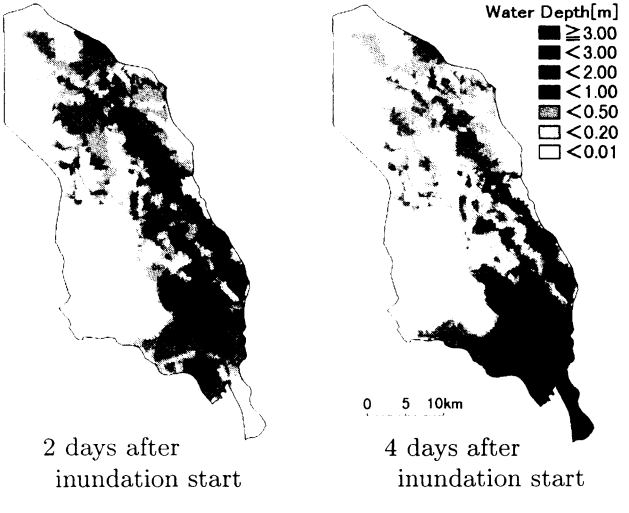

Figure 9: Temporal change of water depth (unstructured meshes)

Hydraulic Engineering Software VIII, C.A. Brebbia & W.R. Blain (Editors)

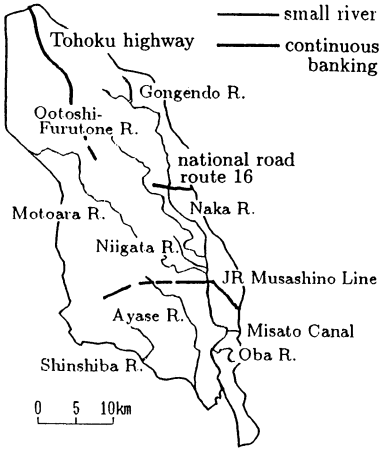

Figure 10: Small rivers and continuous banking

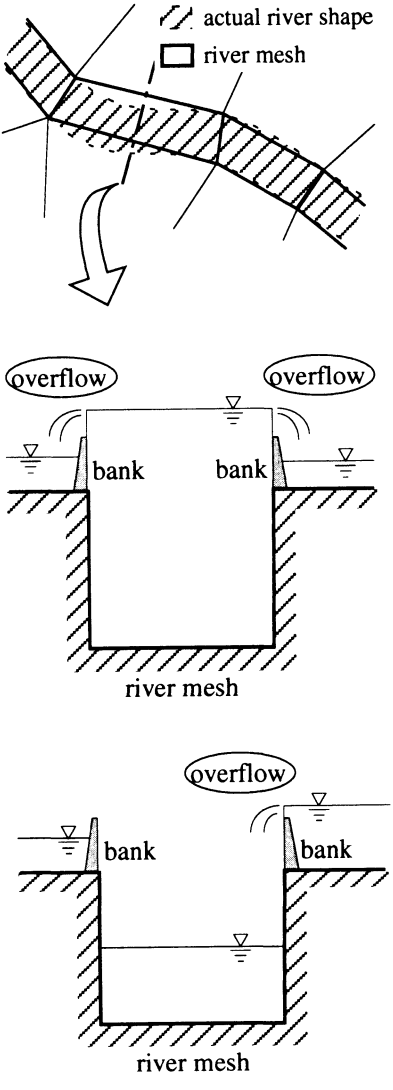

Figure 11: Treatment of river mesh

and the neighboring surface elevation data. For the river bank, the assumed wall with bank crown height is imposed at the border adjacent to river meshes and neighboring flood plain meshes. Also, between the river mesh and the flood plain mesh, the following overflow formula [3] is applied. Assuming that for the adjacent two meshes, the lower water stage is h_l, the higher water stage is h_h and the bank crown elevation is h_0 and $h_1 = h_h - h_0$ and $h_2 = h_l - h_0$, the discharge flux M_0 for $h_1 > 0$ is given as follows;

$h_2/h_1 < 2/3$ (perfect overflow);

$$M_0 = \mu h_1 \sqrt{2gh_1} \tag{9}$$

$h_2/h_1 > 2/3$ (submerged overflow);

$$M_0 = \mu' h_2 \sqrt{2g(h_1 - h_2)} \tag{10}$$

where μ and μ' are the discharge coefficient for perfect overflow and submerged overflow, respectively and the values are 0.35 and 0.91, respectively.

Hydraulic Engineering Software VIII, C.A. Brebbia & W.R. Blain (Editors)

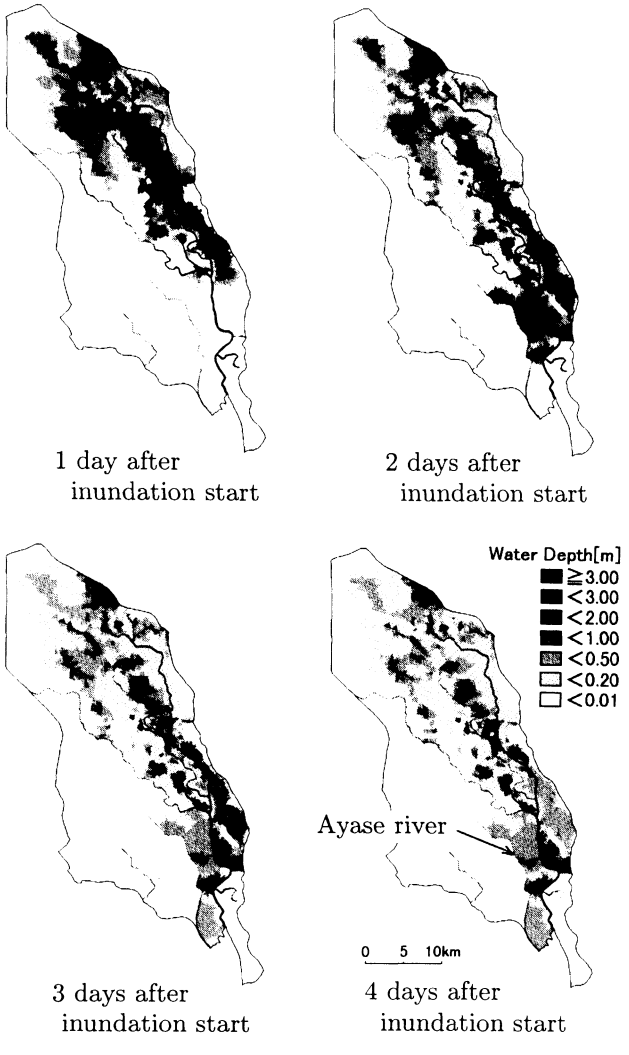

Figure 12: Temporal change of water depth (considering small rivers)

Manning coefficient n is 0.02 for the river meshes and 0.067 for the flood plain meshes. The treatment of river mesh and bank is shown in Figure 11. As for the boundary condition, the inundation water drainage is considered only at the downstream ends of the Naka river, the Ayase river, the Shinshiba river and the Misato channel, where the outflow discharges are expressed by the uniform flow condition by Manning equation. Meanwhile,

Hydraulic Engineering Software VIII, C.A. Brebbia & W.R. Blain (Editors)

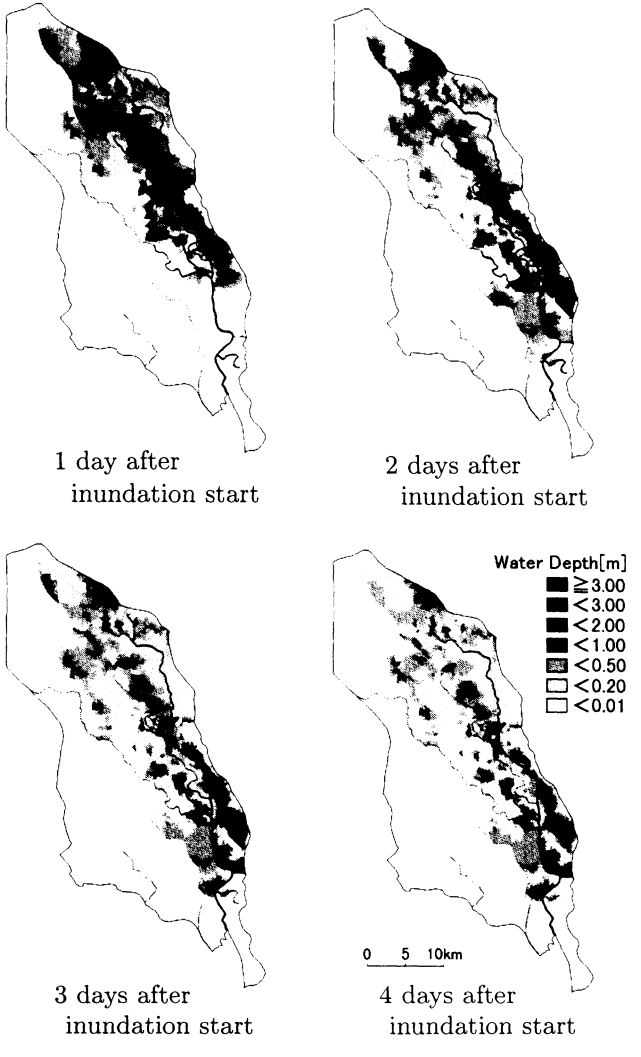

Figure 13: Temporal change of water depth
(considering small rivers and continuous bankings)

the other boundary is assumed to be surrounded by a high wall. As for the initial condition of the rivers, the non-uniform flow computation results for the assumed flood discharges are used. The discharges in the above are also imposed as the river discharges during the inundation computation period.

The results obtained under the above conditions are shown in Figure 12. It is easily understood that by the comparison with Figure 9, the in-

undation depth near the river downstream area is much reduced, and the inundation area extension is interrupted by the left bank of the Ayase river. The record in flooding in 1947 shows that the inundation area is limited in the left bank sides of the Motoara river and the Ayase river. The computed result gives a good agreement with this record except for the downstream area of the Misato channel in the left bank side of the Naka river. The inundation flow characteristics that inundation flow is drained through the rivers in the studied area and it is dammed up and interrupted by the river banks can be well expressed by this model.

In addition to the small rivers, the computation considering the continuous banking such as railway and road is also executed. The continuous bankings of Tohoku highway, national road route 16 and JR Musashino line in Figure 10 are incorporated and the discharge fluxes passing these bankings are computed by eqns (9) and (10) similarly with the case considering the river banks only. The computed results are shown in Figure 13. It is confirmed that the extension of inundation flow area is interrupted by the banking of Tohoku highway in the north-western area. It is also seen that the inundation depth two days after the inundation start is higher in the upstream side of the JR Musashino line banking, and inundation flow is partially stored. Meanwhile, the banking of national road route 16 does not give much influence to the change of inundation flow behavior. This is by the reason that this continuous bank is not so long and that the surrounding surface elevation is comparatively high.

4 Conclusions

From these results, it can be concluded that the inundation flow model developed here based on the unstructured meshes can evaluate the influence of small rivers and continuous banks successfully and this can be applicable enough for inundation flow prediction in urban area.

References

[1] Iwasa, Y. & Inoue, K. Numerical effect of non-linear convective terms on two-dimensional flood flows invasion analysis, *Hydrosoft '84, Hydraulic Engineering Software*, **2**, pp.17-28, 1984.

[2] Kawaike, K., Inoue, K. & Toda, K. Application of unstructured meshes to inundation flow analysis in urban area, *Annual Journal of Hydraulic Engineering*, JSCE, **44**, 2000. (in Japanese, in printing)

[3] JSCE *Hydraulic Formulae*, p.265, 1971. (in Japanese)